

PACS numbers: 42.65.Ky; 42.65.Yj; 42.65.Tg; 05.45.–a
DOI: 10.1070/QE2010v040n07ABEH014311

Optimal feedback in efficient ring double-cavity optical parametric oscillators

V.M. Petnikova, V.V. Shuvalov

***Abstract*. It is shown that the use of two feedback circuits with matched transfer constants and optimal phase incursions in a nondegenerate optical parametric oscillator (OPO) makes it possible to localise the extremes of intensity distributions of interacting waves on the output face of a nonlinear crystal, which provides maximum possible conversion efficiency of pump energy. The optimisation procedure in this case is rather flexible because it is reduced to ambiguous matching of the period and shift of the extremes of exact analytic solutions of the corresponding problem in the form of cnoidal waves with respect to the nonlinear crystal position. Unlike the single-cavity OPO scheme, both these parameters can substantially exceed the nonlinear crystal length and even tend to infinity, which corresponds to solitary soliton-like solutions.**

Keywords: *double-cavity optical parametric oscillator, period and shift of the extremes of cnoidal waves, optimisation of transfer constants of feedback circuits.*

1. Introduction

The authors of paper [1] showed that the problem of nonlinear interaction of three collinear plane monochromatic waves – modes with the frequencies ω_1, ω_2 and $\omega_3 = \omega_1 + \omega_2$ – in a quadratic-nonlinear medium [2] can be solved by increasing the order of the system of truncated equations. In this case, the problem is reduced to three independent ordinary differential second-order equations coupled only by boundary conditions and coinciding in form with the stationary nonlinear Schrödinger equations. This allows one to describe the competition of processes of quantum merging ($\omega_1 + \omega_2 \to \omega_3$) and decomposition ($\omega_3 \to \omega_1 + \omega_2$) in terms of the effective cascade cubic Kerr-type nonlinearity [3]. In paper [4], the same approach was used to analyse the processes proceeding in the case of cascade parametric frequency conversion. Papers [5, 6] present the solutions describing the parametric generation of light (including cascade generation) in a scheme of a travelling-wave generator in which the feedback is absent and, therefore, a weak input noise is parametrically amplified in a nonlinear crystal. In paper [7], this approach was used to optimise the scheme of a single-cavity optical parametric oscillator (OPO) [8]. It was shown that within the framework of this description the use of a feedback decreases the period of cnoidal waves being produced in a nonlinear crystal [1, 4, 9] and optimisation of its transfer constant (reflectivity of the output mirror of the cavity) is reduced to matching the period of cnoidal waves with the nonlinear crystal length.

Below, we will consider the problem of optimisation of double-cavity OPOs. To our knowledge, an exact (from the viewpoint of abandonment of approximation of the given pump field) analytic solution of such problems was presented only for the case of generation of so-called subharmonics [8], i.e., for situations in which $\omega_1 = \omega_2$ and the photons generated in a nonlinear crystal are indiscernible. Using the above-described approach, we will show that in the absence of absorption the use of two feedback loops with matched transfer coefficients makes it possible to localise the cnoidal wave extremes produced on the output face of a nonlinear crystal, which provides realisation of maximally achievable efficiency. The optimisation procedure in this case is rather flexible because it is reduced to matching the period of cnoidal waves and shift of cnoidal wave extremes with respect to the nonlinear crystal position. Both these parameters can markedly exceed the nonlinear crystal length and even tend to infinity (in the regime of formation of solitary soliton-like solutions).

2. Basic equations

As in paper [7], consider collinear interaction of plane monochromatic waves: two waves – at the fundamental frequency (amplitudes $A_{1,2}$, frequencies $\omega_{1,2} = \omega$, wave vectors $\boldsymbol{k}_{1,2}$) and one wave – at the second harmonic frequency (amplitude A_3, frequency $\omega_3 = 2\omega$, wave vector $\boldsymbol{k}_3$), propagating along the z axis. Neglecting absorption, we assume that the nonlinear crystal occupies the region $0 \leqslant z \leqslant L$ (L is the nonlinear crystal length) and realises nondegenerate (due to orthogonal linear polarisations of modes at frequencies $\omega_{1,2}$) parametric process of the so-called II type. As was shown in [1], this interaction can be described by independent ordinary differential second-order equations, which, in the case $\Delta = k_1 + k_2 - k_3 = 0$ most interesting for OPO realisation, take the form [7]

$$\frac{\mathrm{d}^2 A_{1,2}}{\mathrm{d}z^2} - \beta^2 (4I_{10,20} - 2I_{20,10} + I_{30} - 4A_{1,2}A_{1,2}^*)A_{1,2} = 0, \quad (1a)$$

V.M. Petnikova, V.V. Shuvalov International Laser Center, M.V. Lomonosov Moscow State University, Vorob'evy gory, 119991 Moscow, Russia; e-mail: vsh@vsh.phys.msu.su

Received 9 March 2010
Kvantovaya Elektronika **40** (7) 624 – 628 (2010)
Translated by I.A. Ulitkin

$$\frac{d^2A_3}{dz^2} + 2\beta^2(I_{10} + I_{20} + I_{30} - A_3A_3^*)A_3 = 0, \tag{1b}$$

with boundary conditions

$$A_{1,2}|_{z=0} = A_{10,20}, \quad \left.\frac{dA_{1,2}}{dz}\right|_{z=0} = -i\beta A_{20,10}^* A_{30}, \tag{2a}$$

$$A_3|_{z=0} = A_{30}, \quad \left.\frac{dA_3}{dz}\right|_{z=0} = -i2\beta A_{10}A_{20}. \tag{2b}$$

Here β is the same nonlinear coupling constant as in the initial system of truncated equations in papers [1, 7]; $I_i(z) = A_i(z)A_i^*(z)$ is a variable proportional to the intensity of the ith ($i = 1-3$) mode, which will be called below the intensity; $I_{i0} = I_i(z=0)$.

Because equations (1) are independent, the desired intensities $I_{1-3}(z)$ can be found by solving any equation from (1). However, taking into account the requirement of complete pump depletion ($I_3|_{z=L} = 0$), optimisation can conveniently be performed by determining $I_3(z)$ from (1b), (2b) and by writing with allowance for two integrals [7] (conservation of the energy flux density and Manly–Row relations [2]) the expression

$$I_{1,2}(z) = I_{10,20} + \frac{1}{2}\Big[I_{30} - I_3(z)\Big]. \tag{3}$$

If generation develops from noises at $\Delta = 0$ and $I_3|_{z=L} = 0$, information about real amplitudes of the three modes $X_i(z) = \sqrt{I_i(z)}$ is complete because their phases $\varphi_i = \varphi_{i0}$ should be constants [1] corresponding to maximal initial (at point $z = 0$) increments of growth $I_{1,2}$ (decrease I_3). Therefore, for φ_{i0} after the substitution $A_i \to X_i \exp(i\varphi_i)$, as in [7], it is easy to obtain the condition $\varphi_{30} = \varphi_{10} + \varphi_{20} + \pi/2$, which we consider below fulfilled although now (unlike [7]) solely due to the optimal choice of phase incursions in feedback circuits. Taking this expression into account, (1b) and (2b) can be written in the final form:

$$\frac{d^2X_3}{dz^2} + 2\beta^2(I_{10} + I_{20} + I_{30} - X_3^2)X_3 = 0, \tag{4a}$$

$$X_3|_{z=0} = X_{30} = \sqrt{I_{30}}, \qquad \left.\frac{dX_3}{dz}\right|_{z=0} = -2\beta X_{10}X_{20} = -2\beta\sqrt{I_{10}I_{20}}. \tag{4b}$$

3. Pump depletion and optimal feedback

Providing amplification of noise seeds A_{10} and A_{20} sufficient for efficient conversion of pump radiation into radiation at the frequencies $\omega_{1,2}$ at reasonable values of the parameters β, L and I_{30} is usually impossible. For this reason, additional feedback circuits are embedded in OPOs [8]. Optimisation of a single-cavity OPO scheme, in which the feedback loop closes only for one of the generated waves, was dealt with in [7] within the framework of the described approach. Below we will consider the peculiarities of double-cavity OPOs [8] and will introduce, unlike [7], two independent (with account for the equality $\omega_1 = \omega_2$ – polarisation-selective) feedback circuits by assuming that some fractions $|R_{1,2}|^2$ of output (at point $z = L$) intensities $I_{1,2}(L)$ of the waves generated in the nonlinear crystal return again to its input (to plane $z = 0$, Fig. 1). Here, $R_{1,2}$ are the complex transfer constants of the fields $A_{1,2}$ from the nonlinear crystal output to its input. Recall that the phase incursions in both circuits are assumed optimal and, therefore, the introduced feedback is positive. Note also that the ring cavity scheme best suits the approximations employed because the interaction of modes at the frequencies $\omega_{1,2}$, which would appear during the backward trip for radiation through the nonlinear crystal in a linear cavity [8], is neglected here.

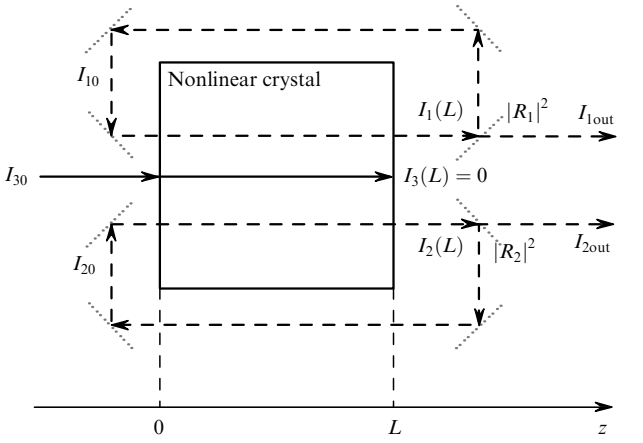

Figure 1. Scheme for calculating a double-cavity OPO.

It is natural to assume that under optimal conditions the pump wave is completely depleted and $I_3(L) = X_3^2(L) = 0$ for the nonlinear crystal length L. Therefore, taking into account the above definitions, $|R_{1,2}|^2 = I_{10,20}/I_{1,2}(L)$, we find from (3) that under these conditions

$$I_{10,20} = \frac{1}{2}\frac{|R_{1,2}|^2}{1 - |R_{1,2}|^2}I_{30}, \quad I_{1,2}(L) = \frac{1}{2}\frac{1}{1 - |R_{1,2}|^2}I_{30}, \tag{5}$$

and the output intensities I_{1out} and I_{2out} of the signal and idle waves, respectively, after the cavity mirrors prove identical

$$I_{1out,2out} = (1 - |R_{1,2}|^2)I_{1,2}(L) = \frac{1}{2}I_{30}, \tag{6}$$

and specified by the law of conservation of the total energy flux and Manly–Row relations.

Because equation (4a) coincides in form with the nonlinear Schrödinger equation for Kerr nonlinearity of defocusing type and $X_3(L) = 0$, the required solution $X_3(z)$ should [9] be proportional to elliptic Jacobi function $\mathrm{sn}(\gamma z, k)$ [10] shifted along the z axis so that the zero of this function be localised at point $z = L$, i.e.,

$$X_3 = X_{3\max}\mathrm{sn}[\gamma(L - z), k], \quad I_3 = I_{3\max}\mathrm{sn}^2[\gamma(L - z), k]. \tag{7}$$

Boundary conditions (4b), taking (5) into account, are rewritten in the form

$$X_{3\max}\mathrm{sn}(\gamma L, k) = \sqrt{I_{30}},$$

$$\gamma X_{3\max}\mathrm{cn}(\gamma L,k)\mathrm{dn}(\gamma L,k) \tag{8}$$

$$=\beta\left[\frac{|R_1|^2|R_2|^2}{(1-|R_1|^2)(1-|R_2|^2)}\right]^{1/2} I_{30}.$$

Here, k is the modulus of the elliptic Jacobi functions $\mathrm{sn}(\gamma z,k)$, $\mathrm{cn}(\gamma z,k)$ and $\mathrm{dn}(\gamma z,k)$ [10], and the numerical values of the parameters γ, k, $X_{3\max}=\sqrt{I_{3\max}}$ and $|R_{1,2}|^2$ should be chosen as to satisfy equation (4a) and boundary conditions (8).

The above requirements with allowance for (3) determine three types of possible solutions of the problem. At $|R_1|^2<|R_2|^2$, we obtain the solution

$$I_1(z)=\frac{1}{2}\frac{I_{30}}{1-|R_1|^2}\mathrm{cn}^2[\gamma(L-z),k],$$

$$I_2(z)=\frac{1}{2}\frac{I_{30}}{1-|R_2|^2}\mathrm{dn}^2[\gamma(L-z),k], \tag{9}$$

where

$$\gamma^2=\frac{\beta^2 I_{30}}{1-|R_2|^2};\quad k^2=\frac{1-|R_2|^2}{1-|R_1|^2};$$

$$I_{3\max}=\frac{I_{30}}{1-|R_1|^2};\quad \mathrm{sn}^2(\gamma L,k)=1-|R_1|^2. \tag{10}$$

At $|R_1|^2>|R_2|^2$, subscripts 1 and 2 in (9) exchange places. The point $|R_1|^2=|R_2|^2=|R|^2$ is a singularity because periodic solutions (7) and (9) become solitary ($k=1$):

$$I_3=I_{3\max}\tanh^2[\gamma(L-z)],$$

$$I_{1,2}(z)=\frac{1}{2}\frac{I_{30}}{1-|R|^2}\cosh^{-2}[\gamma(L-z)], \tag{11}$$

where

$$\gamma^2=\frac{\beta^2 I_{30}}{1-|R|^2};\ I_{3\max}=\frac{I_{30}}{1-|R|^2};$$

$$\tanh^2(\gamma L)=1-|R|^2, \tag{12}$$

which coincides with the degenerate case (sub-harmonic generation) considered in [8].

4. Optimal ratio of transfer constants

It follows from (10) that at $|R_1|^2\neq|R_2|^2$ the condition of complete pump-wave depletion $[I_3(L)=0]$ relates the optimal transfer constants $|R_1|^2$ and $|R_2|^2$ of two feedback circuits by a transcendental equation

$$\mathrm{sn}\left[\beta\left(\frac{I_{30}}{1-|R_{\max}|^2}\right)^{1/2}L,\left(\frac{1-|R_{\max}|^2}{1-|R_{\min}|^2}\right)^{1/2}\right]$$

$$=(1-|R_{\min}|^2)^{1/2}, \tag{13}$$

where $|R_{\max,\min}|^2=\max,\min|R_{1,2}|^2$. Solutions (13) can be conveniently analysed graphically (Fig. 2). To this end, we will solve equation (13) with respect to the parameter $\beta\sqrt{I_{30}}L$, whose value is given only by the characteristics of the nonlinear crystal (βL) and pump (I_{30}), by writing an equality

$$\beta\sqrt{I_{30}}L=F(|R_1|^2,|R_2|^2)=(1-|R_{\max}|^2)^{1/2}$$

$$\times\int_0^{(1-|R_{\min}|^2)^{1/2}}\left(1-\frac{1-|R_{\max}|^2}{1-|R_{\min}|^2}\xi^2\right)^{-1}\frac{\mathrm{d}\xi}{1-\xi^2}, \tag{14}$$

where $F(x,y)$ is some 'standard' (because it is proportional to the incomplete elliptic integral of the first kind) function, which is symmetric with respect to the permutation of the arguments $x\leftrightarrow y$. It means that equation (14) determines the standard surface in the space $(|R_1|^2,|R_2|^2,\beta\sqrt{I_{30}}L)$, and the array of points $(|R_1|^2,|R_2|^2)$ localised on the line of intersection of this surface with the plane $\beta\sqrt{I_{30}}L=\mathrm{const}$, specifies a set of pairs of optimal transfer constants $|R_1|^2$ and $|R_2|^2=f_{\beta\sqrt{I_{30}}L}(|R_1|^2)$ of feedback circuits. Here, $f_a(y)$ is the function which is the solution of the equation $a=F(x,y)$. Obviously, all these pairs are matched both with each other ($|R_2|^2$ is the function of $|R_1|^2$ and vice versa) and with the parameters of the converter and its

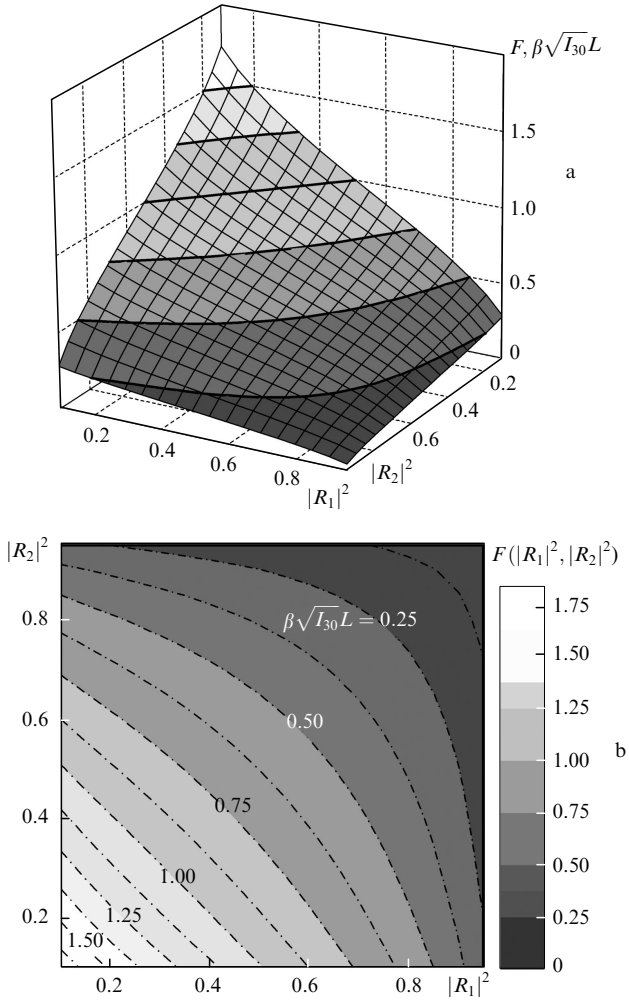

Figure 2. Graphical solution of equation (14): the surface $F(|R_1|^2,|R_2|^2)$ and lines of its intersection with the planes $\beta\sqrt{I_{30}}L=\mathrm{const}$ (a) as well as the dependences $|R_2|^2=f_{\beta\sqrt{I_{30}}L}(|R_1|^2)$ (dash-and-dot curves) and the same surface in the form of a map in the shades of gray (b).

pump (the character of these functions depends on the parameter $\beta\sqrt{I_{30}}L$).

Figure 2a presents the mentioned surface $F(|R_1|^2, |R_2|^2)$ and lines of its intersection with the planes $\beta\sqrt{I_{30}}L = 0.25$, 0.5, 0.75, 1.0, 1.25, and 1.5. Figure 2b shows the character of the dependences $|R_2|^2 = f_{\beta\sqrt{I_{30}}L}(|R_1|^2)$ for the same (as in Fig. 2a) values of the parameter $\beta\sqrt{I_{30}}L$ and the same surface in the form of a map in shades of gray.

Taking into account that что $\omega_1 = \omega_2$, in the limiting case $|R_1|^2 = |R_2|^2 = |R|^2$, the problem being solved becomes degenerate and expression (13) is reduced to the relation known from [8]

$$\tanh\left[\beta\left(\frac{I_{30}}{1-|R|^2}\right)^{1/2}L\right] = (1-|R|^2)^{1/2}, \tag{15}$$

which is easily solved with respect to $\beta\sqrt{I_{30}}L$:

$$\beta\sqrt{I_{30}}L = F_1(|R|^2)$$

$$= \frac{1}{2}\left(1-|R|^2\right)^{1/2}\ln\frac{1+(1-|R|^2)^{1/2}}{1-(1-|R|^2)^{1/2}}. \tag{16}$$

Here, $F_1(|R|^2) = F(|R|^2, |R|^2)$ is also a standard function shown in Fig. 3 by a solid curve. The dashed curve in this figure is the function $F_2(|R|^2) = F(|R|^2, 0)$ corresponding to another limiting situation – single-cavity OPO scheme. One can easily see that in this case expression (13) is transformed into the equation

$$\mathrm{sn}\left[\beta\left(\frac{I_{30}}{1-|R|^2}\right)^{1/2}L, (1-|R|^2)^{1/2}\right] = 1, \tag{17}$$

whose solution

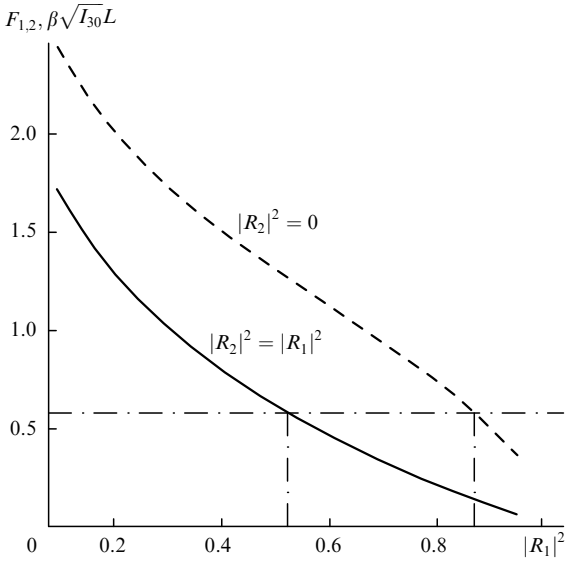

Figure 3. Graphical solution of equations (16) and (18): the dependence $F_1(|R|^2) = F(|R|^2, |R|^2)$ for a double-cavity OPO scheme (solid curve) and the dependence $F_2(|R|^2) = F(|R|^2, 0)$ for a single-cavity OPO scheme (dashed curve). The optimal values of the transfer constants in feedback circuits are determined by the abscissa of points of intersection of the dash-and-dot line $\beta\sqrt{I_{30}}L = \text{const}$ with the two mentioned dependences.

$$\beta\sqrt{I_{30}}L = F_2(|R|^2) = (1-|R|^2)^{1/2}K[(1-|R|^2)^{1/2}] \tag{18}$$

has been already previously derived and analysed in [7]. Here, $K(k)$ is the complete normal elliptic Legendre integral of the first kind [10].

The optimal transfer constants in these two limiting cases can be also found graphically (Fig. 3). At the given $\beta\sqrt{I_{30}}L$, the same maximal OPO efficiency (6), as in the single-cavity scheme, can be realised by using two feedback circuits with identical ($|R_1|^2 = |R_2|^2$) but significantly smaller transfer constants (Fig. 3). This circumstance is a matter of principle. The fact is that elsewhere previously, as in [7], the stationary problem was solved, i.e., the regime of the established generation was analysed. In practice, during some time after switching on the pump, the feedback is not optimal because of a transient process proceeding in the system, which is caused by the formation of optimal input fields – seeds ($I_{10,20}$).

The dynamics of this process in the case of instantaneous [$I_{30}(t) = 0$ at $t < 0$ and $I_{30}(t) = I_{30}$ at $t \geqslant 0$] switching on of the pump, calculated by the method of successive time steps [8], is illustrated in Fig. 4. One can see that in this example the duration of the transient process in the case of the optimal double-cavity OPO scheme is approximately three times smaller than in the case of the optimal single-cavity scheme. In both situations we can well observe the time interval during which $I_{\text{out}}(t) < 1$ and the pump-wave energy is stored in the cavity (cavities). One more characteristic feature of the optimal single-cavity OPO scheme is its pronounced asymmetry due to which $I_{1\text{out}}(t) > I_{2\text{out}}(t)$ during the entire transient process.

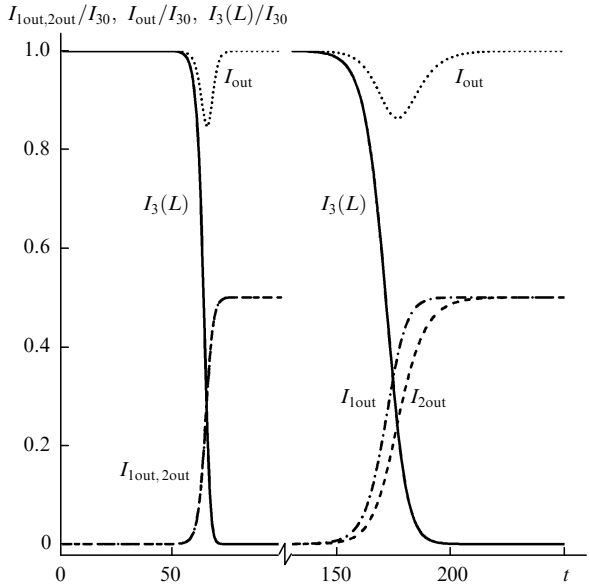

Figure 4. Transient process after instantaneous switching on of the pump: the dependences $I_{1\text{out}}(t)$ (dash-and-dot curves),, $I_{2\text{out}}(t)$ (dashed curves), $I_3(L,t)$ (solid curves) and total energy flux density from the cavity $I_{\text{out}}(t) = I_{1\text{out}}(t) + I_{2\text{out}}(t) + I_3(L,t)$ (dotted curves) normalised to I_{30}. The right side of the figure ($130 \leqslant t \leqslant 250$) corresponds to the optimal single-cavity OPO scheme ($|R_1|^2 = 0.87$ and $|R_2|^2 = 0$), and the left side ($0 \leqslant t \leqslant 100$) – to the optimal double-cavity OPO scheme ($|R_1|^2 = |R_2|^2 = 0.52$) at $\beta\sqrt{I_{30}}L = 0.6$ (see Fig. 3). Time t is normalised to the round-trip transit time for radiation in the cavity, the relative level of input noises is $I_{10,20}(t=0)/I_{30} = 10^{-16}$.

5. Conclusions

We have shown that in the case of nondegenerate parametric generation in the absence of losses, the use of two feedback circuits with matched transfer constants and optimal phase incursions makes it possible to localise the extremes of spatial (with respect to the longitudinal coordinate) intensity distributions of interacting waves on the output face of the nonlinear crystal. The optimisation procedure is rather flexible in this case because it is reduced to one from a set of possible matching of the period and shift of the extremes of analytic solutions of the corresponding problem in the form of cnoidal waves with respect to the nonlinear crystal position. Unlike the single-cavity OPO scheme, both these parameters can significantly exceed the nonlinear crystal length and even tend to infinity, which corresponds to realisation of solitary soliton-like solutions.

During some time after switching on the pump, such a feedback is not optimal because of a transient process proceeding in the system, which is caused by the formation of the required input fields – seeds. The duration of the transient process in the optimal double-cavity OPO scheme proves much shorter than in the single-cavity scheme.

Note that as far as we know, the exact (from the viewpoint of abandonment of approximation of the given pump field) analytic solution of such problems was presented only for the degenerate case of generation of subharmonics [8], i.e., for situations in which the photons generated at the frequencies $\omega_{1,2}$ in a nonlinear crystal are indiscernible. Note also that in the absence of dispersion, a simple change of variables [8] in the synchronous interaction under study can easily take into account the distributed losses introduced by the nonlinear crystal.

References

1. Petnikova V.M., Shuvalov V.V. *Phys. Rev. E*, **76** (4), 046611 (2007).
2. Akhmanov S.A., Khokhlov R.V. *Problems of Nonlinear Optics* (New York: Gordon and Breach, 1972; Moscow: VINITI, 1964); Bloembergen N. *Nonlinear Optics* (New York: Benjamin, 1965; Moscow: Mir, 1966).
3. Ostrovskii L.A. *Pis'ma Zh. Eksp. Teor Fiz.*, **5** (9), 331 (1967); Klyshko D.N., Polkovnikov B.F. *Kvantovaya Elektron.*, 4 (16), 81 (1973) [*Sov. J. Quantum Electron.*, **3** (4), 324 (1973)]; Meredith G.R. *J. Chem. Phys.*, **77** (12), 5863 (1982); Kobyakov A., Lederer F. *Phys. Rev. A*, **54** (4), 3455 (1996).
4. Petnikova V.M., Shuvalov V.V. *Phys. Rev. E*, **79** (2), 026605 (2009).
5. Petnikova V.M., Shuvalov V.V. *Kvantovaya Elektron.*, **40** (3), 219 (2010) [*Quantum Electron.*, **40** (3), 219 (2010)].
6. Petnikova V.M., Shuvalov V.V. *Kvantovaya Elektron.*, **40** (4), 329 (2010) [*Quantum Electron.*, **40** (4), 329 (2010)].
7. Petnikova V.M., Shuvalov V.V. *Kvantovaya Elektron.*, **40** (7), 619 (2010) [*Quantum Electron.*, **40** (7), 619 (2010)].
8. Dmitriev V.G., Tarasov L.V. *Prikladnaya nelineinaya optika: Generatory vtoroi garmoniki i parametricheskie generatory sveta* (Applied Nonlinear Optics: Second Harmonic Generators and Optical Parametric Oscillators) (Moscow: Radio i svyaz', 1982).
9. Petnikova V.M., Shuvalov V.V., Vysloukh V.A. *Phys. Rev. E*, **60** (1), 1009 (1999).
10. Gradshteyn I.S., Ryzhik I.M. *Tables of Integrals, Series, and Products* (New York: Acad. Press, 2000; Moscow: Nauka, 1989); Kuznetsov D.S. *Spetsial'nye funktsii* (Special Functions) (Moscow: Vyssh. shk., 1965); Abramowitz M., Stegun I.A. (Eds) *Handbook of Mathematical Functions with Formulas, Graphs, and Mathematical Tables* (New York: Dover Publications, 1972; Moscow: Nauka, 1979).